

# Specimen Geometry Effect on the Mechanical Properties of AISI 1040 Steel

Adnan Calik<sup>a</sup>, Osman Sahin<sup>b,c</sup>, and Nazim Ucar<sup>b</sup>

<sup>a</sup> Department of Mechanical Education, Technical Education Faculty, Suleyman Demirel University, Isparta, Turkey

<sup>b</sup> Physics Department, Art and Science Faculty, Suleyman Demirel University, Isparta, Turkey

<sup>c</sup> Present address: Physics Department, M. Kemal University, Hayat, Turkey

Reprint requests to N. U.; E-mail: nazmucar@yahoo.com

Z. Naturforsch. **63a**, 448–452 (2008); received January 11, 2008

The specimen geometry effect on some mechanical properties, such as tensile behaviour and hardness, of borided and unborided AISI 1040 steels was investigated. Boronizing of steels was performed by the powder pack method at 1210 K for 4 h. The specimen geometry and the boride layer thickness and hardness is similar for all tested boronized steels and independent of varying the shape of cross-sections. On the other hand, the ultimate tensile stress and elongation depend on the specimen geometry due to stress concentration at the corners of the specimen.

*Key words:* Boronizing; Borides; Microhardness; Ultimate Stress; Cracks.

## 1. Introduction

Boronizing is a thermochemical surface hardening process that enriches the material surface with boron atoms by diffusion of the atoms into the surface at high temperatures. According to many researchers [1–3], coatings applied to surfaces have the ability to modify their static and dynamic mechanical properties. Boronized steels are characterized by increased surface hardness and increased wearing resistance [4–6]. On the other hand, when ferrous-based materials are boronized at temperatures of 800–1000 °C for 1 to 8 h, Fe<sub>2</sub>B + FeB or Fe<sub>2</sub>B iron-boride phases are formed, and a boride layer having up to 2000 HV hardness is produced [7–9].

Considering the plastic deformation of materials and understanding the effects of specimen size and geometry on the mechanical properties of boronized and unboronized samples is important for realizing their widespread use in aerospace and civil infrastructures. Although the literature is full of experimental and theoretical studies investigating the material behaviour under compressive and tensile loads along different material axes, few have addressed the size effect systematically [10]. Corresponding to this, specimen geometry effects on the mechanical properties of materials have been studied in metallic glasses [11]. It has been shown that the specimen geometry effects are closely related to the constraint of shear band processes and deforma-

tion processes, resulting in various mechanical properties. On the other hand, Zdunek et al. [12] showed that the Portevin-Le Chatelier (PLC) effect, in the form of serrations on stress-strain curves, depends on the geometry of specimen cross-sections, and the obtained results provide a new insight into the dynamics of the PLC effects. Recently, Vorob'ev [13] reported that the deformability of boronized steels is related to the geometry of the test object, whereas the character of this relation is determined by the test temperature and class of steel. Finally, it has been concluded that the observations and the further understanding of the specimen geometry effect on the mechanical properties will help to understand the deformation and fracture mechanism, and thus improve the mechanical properties of materials. In the present study we examined the characteristics of tensile and hardness properties depending on the specimen geometry of borided and unborided AISI 1040 medium carbon steels.

## 2. Experimental

The substrates used for this study were AISI 1040 mold steels. Boriding of the steels was achieved in a solid medium using the powder pack method. In this method, the commercial Ekabor-II boron source and activator (ferrosilicon) were thoroughly mixed to form the boriding packet. The test samples and packet were heated in an electrical resistance furnace for 4 h at

1210 K under atmospheric pressure. After this process, borided samples were removed from the furnace and cooled in air. Borided samples were sectioned from one side and metallographically prepared up to 1200-grid emery paper, and then polished using 0.3- $\mu\text{m}$  alumina pastes. Polished samples were etched by 4% Nital before tests. To investigate specimen geometry effects on the mechanical properties of AISI 1040 steels, borided and unborided specimens were cut out of the same piece of material. The specimens have the same amount of length and the same cross-section area, but varying shape of cross-sections (circular, square, rectangular) as indicated by Zdunek *et al.* [12]. Thus, the geometric factor (GF) was defined as area of cross-section to perimeter ratio for each specimen. The presence of borides formed in the coating layer was confirmed by means of X-ray diffraction (XRD) and optical microscopy. Also, the boride layer thickness and distribution of alloying elements from the surface to the interior were determined by optical microscopy and energy dispersive X-ray spectroscopy (EDS), respectively.

Borided and unborided steels were pulled with an Instron type machine at a strain rate of  $10^{-6} \text{ s}^{-1}$  and room temperature. Load and elongation curves were recorded during the tensile tests and were converted into stress-strain curves. To determine the hardness of the borided steels a Vickers microhardness tester with a load of 100 g was used. Many indentations were made on each coating film under each experimental condition to check the reproducibility of hardness data.

### 3. Results and Discussion

It is well known that a boride layer on the upper surface of a specimen forms as a result of boron diffusion into the surface during the boronizing process. Figure 1 shows an optical microstructure of a cross-sectional view of boronized AISI 1040 steels. Optical microscopy studies on borided steels with the same cross-section area and varying cross-section shape showed that borides formed on the surface of steels have a saw-tooth morphology and a uniform coating thickness. Moreover, three distinct regions were identified on the surface of steels: (i) borides, (ii) transition zone, and (iii) matrix. It was observed that the prominent phase formed on the surface of AISI 1040 steels was  $\text{Fe}_2\text{B}$ , which was revealed by XRD and EDS analysis (Figs. 2 and 3). It has to be noticed that the formation of a single phase with saw-tooth morphology is

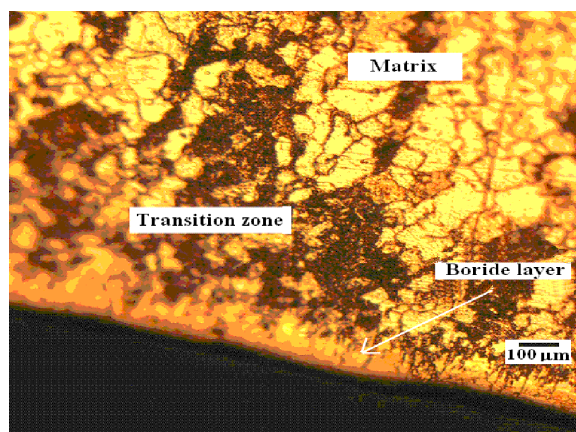


Fig. 1. Optical microscope cross-sectional view of borided AISI 1040 steel.

needed for industrial applications because of superior wear resistance and mechanical properties [14]. In the specimens made of AISI 1040 steels, the boride layer thickness varied between 90 and 100  $\mu\text{m}$ . Moreover, the thickness of the transition zone is very small (average 150  $\mu\text{m}$ ), and it displays an improvement of the fine grained structure (Fig. 1). This is because the carbon does not dissolve significantly in the boride layer during boronizing. Microhardness measurements were carried out from the surface to the interior along a line to see the variation of the hardness of the boride layer, transition zone and matrix, respectively. While microhardness values in the non-borided specimens and matrix varied between 280 HV0.1 and 290 HV0.1, they reached 310–320 HV0.1 and 1530–1580 HV0.1 in the transition zone and boride layer, respectively. It can easily be seen that the microhardness values of the boride layer are higher than of the matrix because of the presence of a hard  $\text{Fe}_2\text{B}$  phase. In [15–17], it has been found that the microhardness and thickness of the boride layer depend on the treatment temperature and time. In the present study, no difference in the effect of specimen geometry on the boride layer thickness and the microhardness were established for boronized AISI 1040 steels with the same cross-section area and varying cross-section shape. From the present results, a decisive conclusion is obtained that the diffusion of boron atoms into the surface is not effected from the specimen geometry.

In order to investigate the specimen geometry effect on the stress-strain behaviour of boronized and unboronized AISI 1040 steels, the room temperature tensile behaviour was also studied. As can be seen from

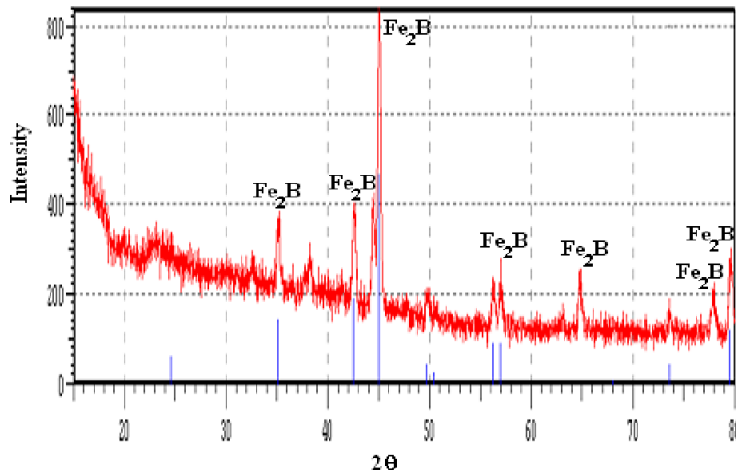


Fig. 2. XRD pattern of AISI 1040 steel borided at 1210 K for 4 h.

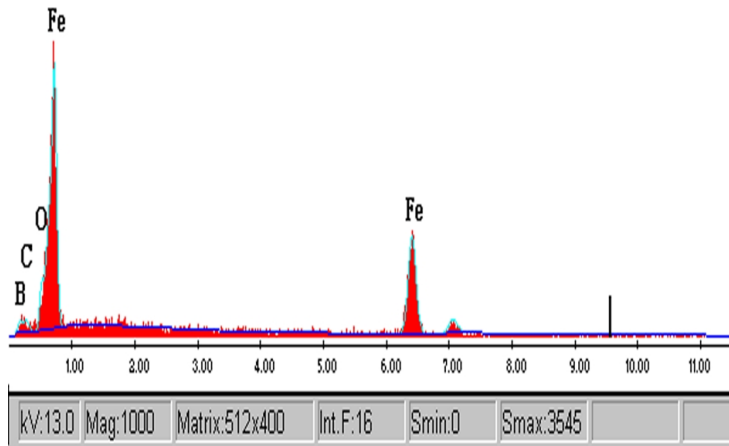


Fig. 3. EDS spectrum of AISI 1040 steel borided at 1210 K for 4 h.

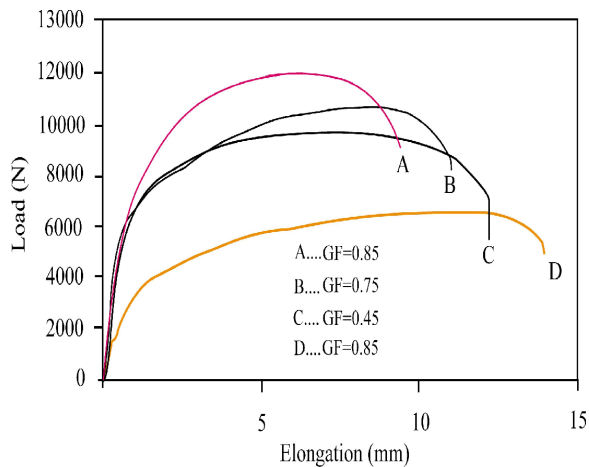


Fig. 4. Load-elongation curves for circular (A), square (B) and rectangular (C) cross-sections of AISI 1040 steel borided at 1210 K for 4 h. D represents unborided AISI 1040 steel having circular cross-sections.

Fig. 4, the well-known shapes were obtained for all steels. The stress-strain curves were calculated from load-elongation curves. The ultimate stress or the yield stress (stress at 0.2% offset strain) obtained from these curves of boronized steels is higher than that of unboronized steels due to the volume thermal treatments and also surface modification as expected by considering the plastic deformation of the materials (Fig. 4). It is also evident from Fig. 4 that the ultimate tensile stress increases as the GF increases for borided specimens with the same cross-section area and varying shape of the cross-section as circular, square and rectangular. By contrast, the uniform elongation decreases with increasing GF as shown in Figure 4. Previous studies [18, 19] have shown that the compressive strength increases noticeably as the size of specimen decreases in the case of cubes, whereas for cylinders the effect of size is almost negligible. Also, it has been found that the post-peak behaviour of the

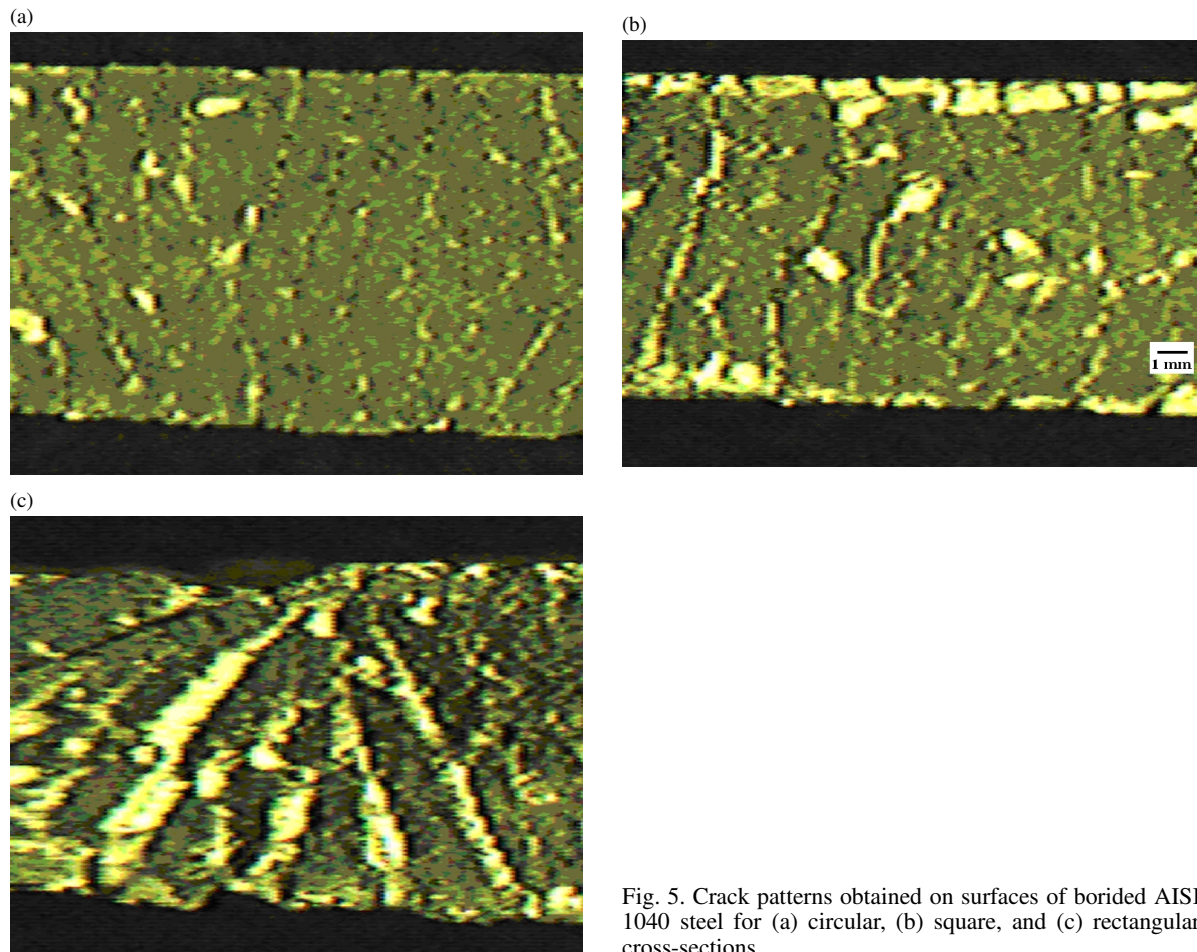


Fig. 5. Crack patterns obtained on surfaces of borided AISI 1040 steel for (a) circular, (b) square, and (c) rectangular cross-sections.

cubes is milder than that of the cylinders, which results in a strong energy consumption after that peak. This behaviour has been explained with crack patterns. It was shown that the extent of cracking throughout the specimen is denser in the cubes than in the cylinders [18]. So, it was concluded that large specimens resist more in terms of stress than smaller ones. We think that the tensile stress behaviour can also be explained with the crack patterns. By comparing optical photographs obtained from the surface of boronized and also loaded AISI 1040 steels with different shapes of cross-sections, crack patterns of AISI 1040 steels are sensitive to the specimen geometry (Fig. 5). The crack patterns on the surface of steels having circular cross-sections are local, small and thin, whereas those having a rectangular cross-section area extend throughout the surfaces and also have a sharp trace. On the other hand, the edges of

steels having square and rectangular cross-sections display significant deformation due to stress concentration at the corners of the specimen (Figs. 5b and c). To sum up, crack pattern appears to play a significant role in the strength and elongation of borided AISI 1040 steels.

#### 4. Conclusions

The borides formed on the surface of steels have a saw-tooth morphology, and the coating thickness is uniform. Also, three distinct regions were identified on the surface of steels: (i) borides, (ii) transition zone, and (iii) matrix. It was observed that a single phase boride layer,  $Fe_2B$ , formed on the surface of AISI 1040 steels boronized under the same conditions. The ultimate stress of boronized steels is higher than that of unboronized steels.

It has to be noted that there were no specimen geometry effects on the formed coating layer, i. e., their thickness and microhardness were similar. But the investigation results showed that the ultimate stress and elongation depend on the geometry of boronized AISI 1040 steels due to stress concentration at the corners of the specimen.

#### Acknowledgements

The authors would like to acknowledge the BOREN under grand number 2006/33-Ç32-20 for financial support.

- [1] C. Bindal and A. H. Ucisik, *J. Aust. Ceram. Soc.* **34**, 287 (1998).
- [2] P. B. Srinivasan, V. Muthupandi, W. Dietzel, and V. Sivan, *Mater. Design* **27**, 182 (2006).
- [3] A. Calik, O. Sahin, A. E. Ekinci, and N. Ucar, *Z. Naturforsch.* **62a**, 545 (2007).
- [4] J. H. Jun and C. S. Choi, *Mater. Sci. Eng. A* **252**, 133 (1998).
- [5] M. Goune, T. Belmonte, A. Redjaimia, P. Weisbecker, J. M. Fiorani, and H. Michel, *Mater. Sci. Eng. A* **351**, 1 (2003).
- [6] M. Bektes, O. Uzun, A. Akturk, A. E. Ekinci, and N. Ucar, *Chin. J. Phys.* **42**, 733 (2004).
- [7] C. Meric, S. Sahin, B. Bactir, and N. S. Koksall, *Mater. Design* **27**, 751 (2006).
- [8] A. Pertek, *Mater. Sci. Forum* **163**, 6 (1994).
- [9] H. J. Hungar and G. Trute, *Hat Treatment Met.* **2**, 31 (1994).
- [10] D. S. Potter, V. Gupta, and S. Hauert, *Composite Sci. Technol.* **60**, 2525 (2000).
- [11] F. X. Liu, P. K. Liaw, G. Y. Wang, C. L. Chiang, D. A. Smith, P. D. Rack, J. P. Chu, and R. A. Buchanan, *Intermetallics* **14**, 1014 (2006).
- [12] J. Zdunek, W. L. Spychalski, J. Mizera, and K. J. Kurzydowski, *Mater. Characterization* **58**, 46 (2007).
- [13] E. V. Vorob'ev, *Strength Mater.* **34**, 5 (2002).
- [14] H. Uslu, H. Comert, M. Ipek, O. Ozdemir, and C. Bindal, *Materials and Design*, **28**, 1 (2007).
- [15] L. L. Qian and G. A. Stone, *J. Mater. Perform.* **4**, 1 (1995).
- [16] S. Sen, I. Ozbek, U. Sen, and C. Bindal, *Surf. Coat. Technol.* **135**, 173 (2001).
- [17] C. Meric, S. Sahin, and S. S. Yilmaz, *Mat. Res. Bull.* **35**, 2165 (2000).
- [18] J. R. Del Viso, J. R. Carmona, and G. Ruiz, *Cem. Concr. Res.* **38**, 386 (2008).
- [19] Z. P. Bazent and J. Planas, *Fracture and Size Effect in Concrete and Other Quasibrittle Materials*, CRC Press, Boca Raton 1998.